Science Advances
AAAS

advances.sciencemag.org/cgi/content/full/5/9/eaax7946/DC1

Supplementary Materials for

Synthetic networks with tunable responsiveness, biodegradation, and molecular recognition for precision medicine applications

John R. Clegg, Afshan S. Irani, Eric W. Ander, Catherine M. Ludolph, Abhijeet K. Venkataraman, Justin X. Zhong, Nicholas A. Peppas*

*Corresponding author. Email: peppas@che.utexas.edu

Published 27 September 2019, *Sci. Adv.* **5**, eaax7946 (2019)
DOI: 10.1126/sciadv.aax7946

This PDF file includes:

Supplementary Materials

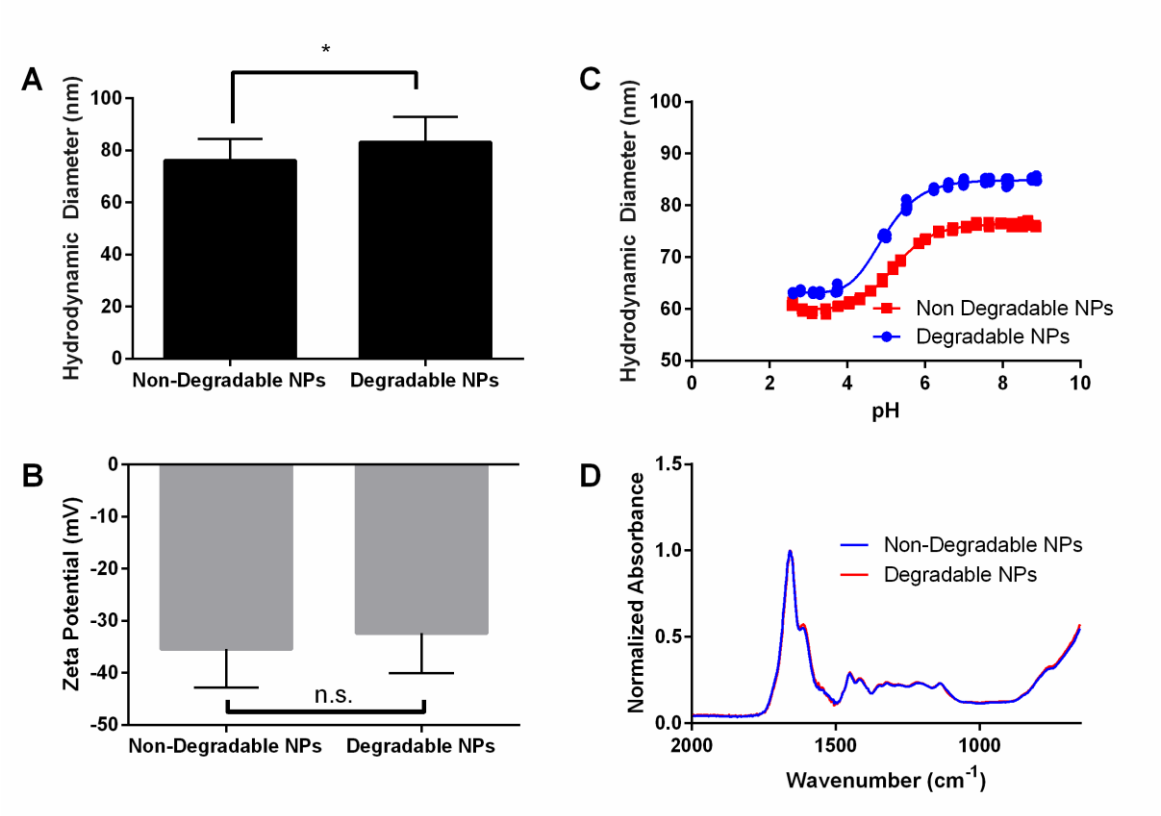

Fig. S1. Proof of similarity for degradable and nondegradable P(AAm-co-MAA) nanogels. (a) Degradable nanogels were slightly larger than their non-degradable analogues. **(b)** No significant differences were observed in the nanogels' zeta potential. **(c)** Degradable and non-degradable nanogels exhibited a similar pH-responsive collapse with a critical transition at pH = 4.8. **(d)** There were no observable differences between the formulations' FTIR spectra, indicating that the compositions are similar. (**a,b**: n = 4 mean ± SD, **c,d**: representative data shown).

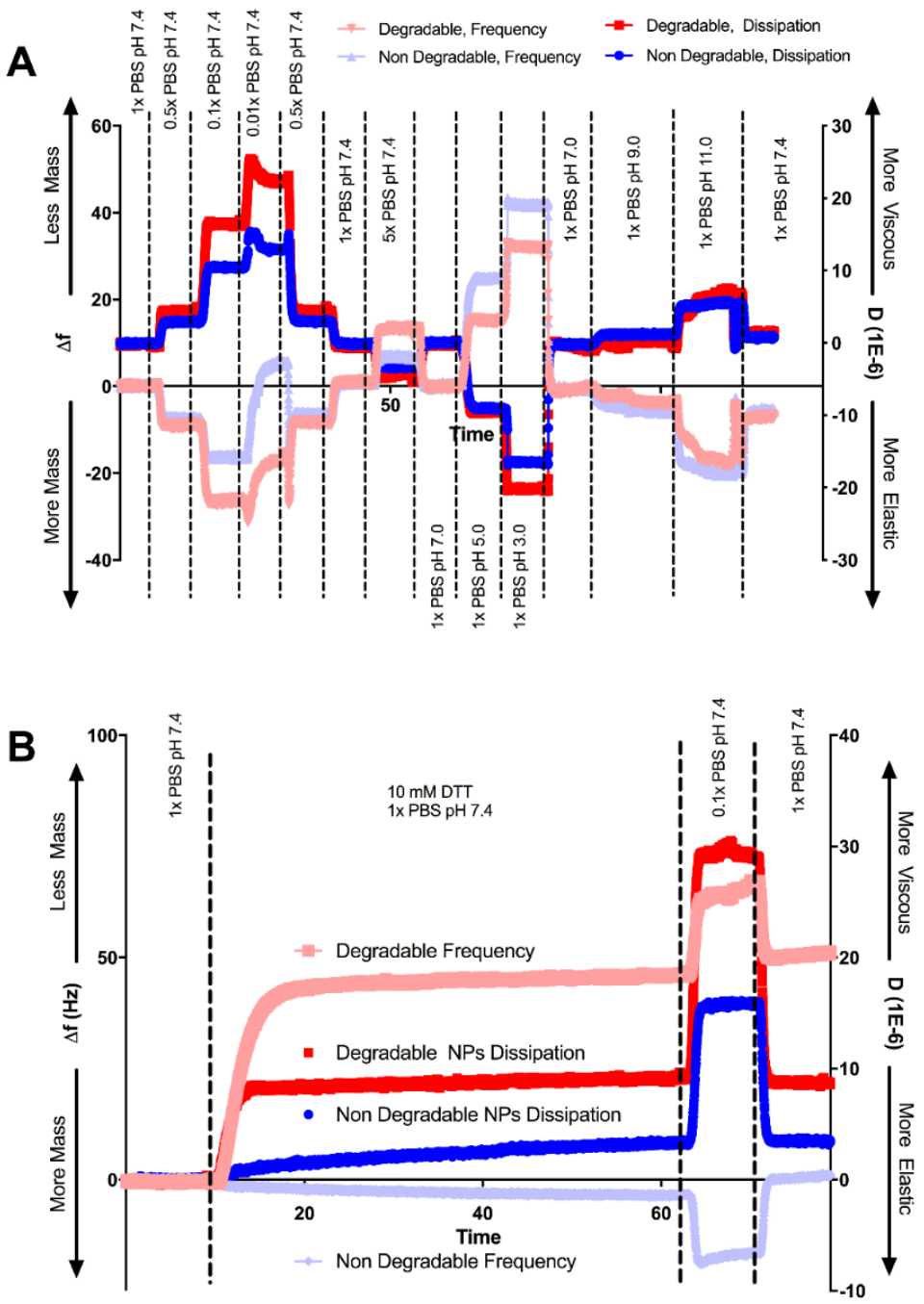

Fig. S2. Nanogel swelling and degradation analysis with QCM. (a) Frequency and dissipation measurements of degradable and non-degradable nanogels in a range of buffer conditions (exploring ionic strength and pH) demonstrated the responsive swelling of the formulations. Swelling presented as a decrease in frequency (i.e. uptake of water mass) and increase in dissipation (increase in viscosity of the polymer nanogel coating). Deswelling presented in an inverse manner (less mass, more elastic). **(b)** Degradable nanogels degraded completely when treated with 10 mM DTT. We knew that the degradation was complete because, when placed in 0.1x PBS buffer (t ~ 65 min), the degraded nanogels simultaneously lost mass and were more viscous. This behavior was consistent with desorption of ions, not swelling of a network (as was observed with the non-degradable gels, that simultaneously increased in mass and viscosity). (n = 4, representative data).

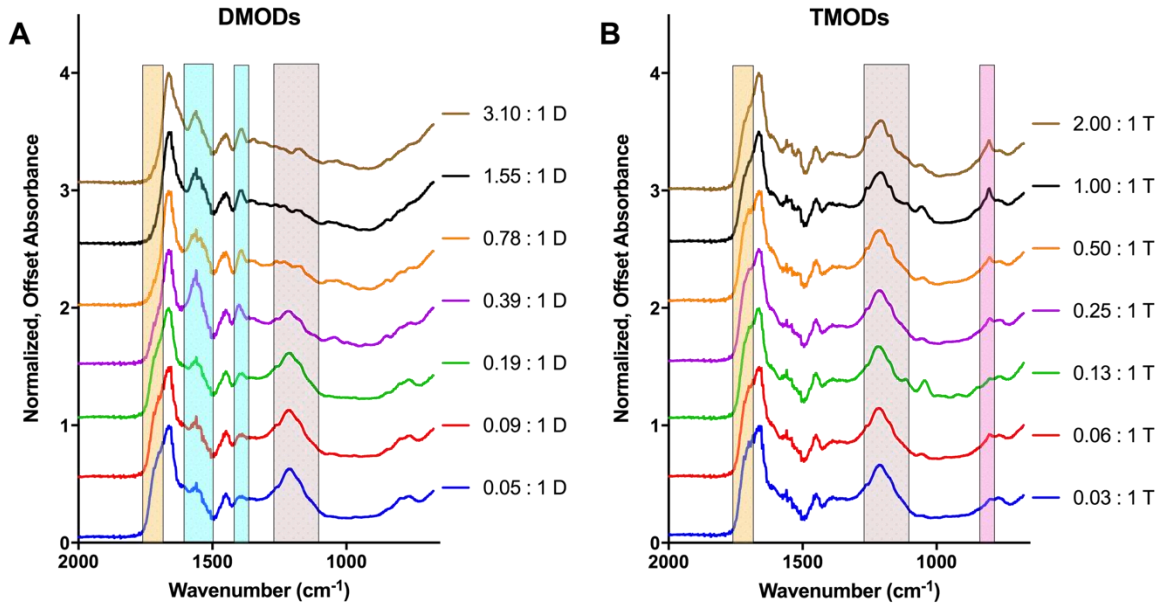

Fig. S3. FTIR analysis of *N,N*-dimethylethylenediamine– or tyramine-conjugated nanogels. FTIR analysis of each modified nanogel formulation confirmed the covalent incorporation of ligand molecules. For comparison, all spectra were normalized to their largest peak, which was the amide carbonyl (from acrylamide, as well as ligand-modified carboxylic acids) for all formulations. The disappearance of the peaks corresponding to the carboxylic acid carbonyl (1700 cm^{-1}) and carbon-oxygen single bond (1200 cm^{-1}) indicated the expected depletion of carboxylic acid groups through modification. Other noteworthy peaks were those at 1590 cm^{-1} and 1400 cm^{-1}, revealing the presence of tertiary amines and 800 cm^{-1}, revealing tyramine's phenol group. The more pronounced depletion of carboxylic acid peaks in the DMOD spectra as compared to TMOD, when taking also into account the known equal efficiency of both modification reactions, indicated that N,N-dimethylethylenediamine modifications occurred preferentially on the nanogel surface, whereas tyramine modifications occurred primarily in the nanogel bulk.

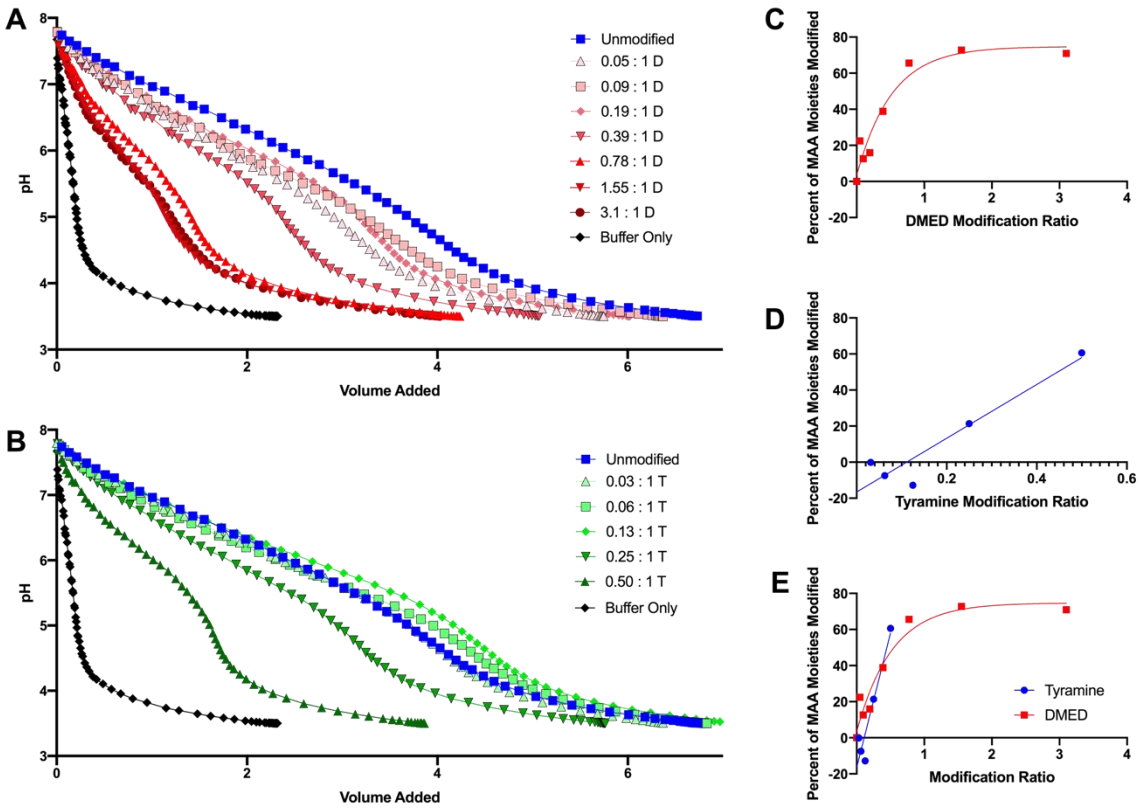

Fig. S4. Potentiometric titration analysis of DMOD and TMOD nanogels. In each spectrum, the extension of the curve (i.e. volume of hydrochloric acid added) revealed the quantity of carboxylic acid groups present. The percent of MAA groups modified was then calculated from the titration curve, and plotted with respect to the stoichiometric ratio of ligand to initial carboxylic acid **(c, d)**. As the ligand ratio increased, the degree of modification increased approximately linearly, up to a plateau observed at approximately 65% modification (for DMOD polymers). We were unable to obtain titration analysis for TMOD polymers with greater extents of modification, as the 1:1 and 2:1 TMOD polymers were not stable in aqueous buffer. Overlay of the TMOD and DMOD titration analysis **(e)** revealed similarity in trend, indicating that the reaction was equally efficient for each ligand. (n = 1).

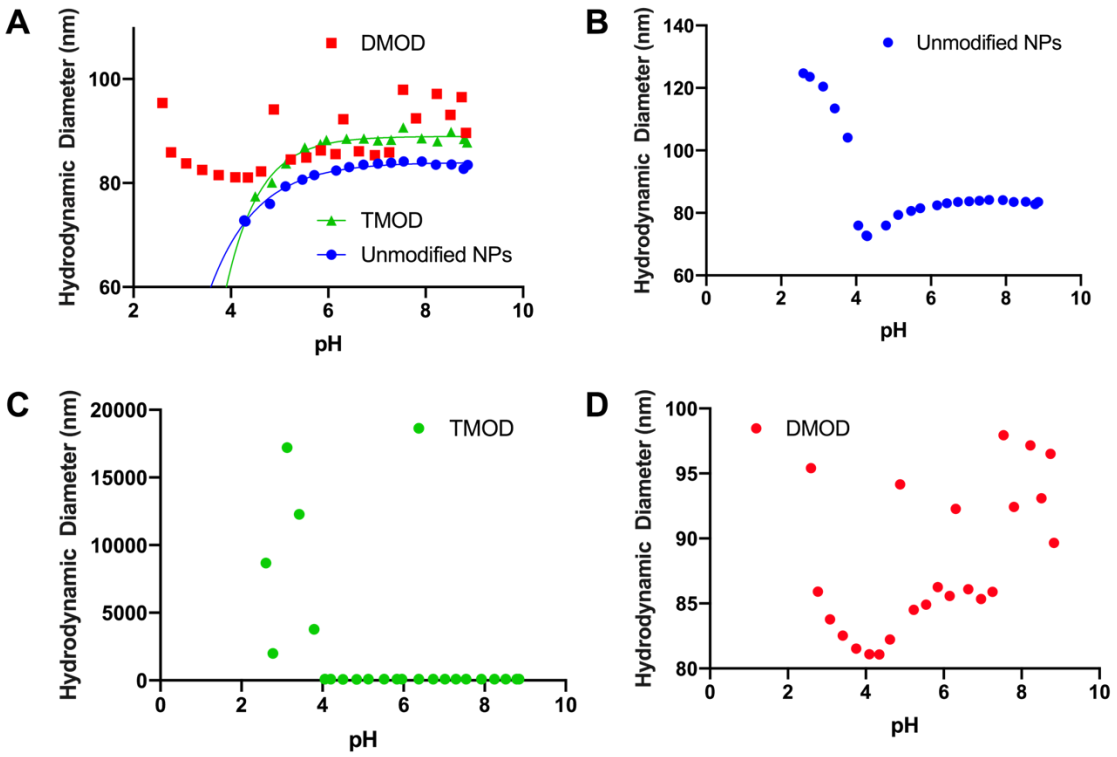

Fig. S5. Full data of pH-responsive, modified nanogel swelling, including data for aggregated nanogels. (a) Overlay of DMOD, TMOD, and unmodified formulations. **(b)** Unmodified nanogels exhibited a pH-responsive collapse with a critical transition at pH ~ 4.8. at pH~4, as the carboxylic acid groups reached greater extents of protonation, the nanogels exhibited minor aggregation. **(c)** 1 to 4 TMOD nanogels aggregated substantially at pH ~4, resulting in micron-scale aggregates. **(d)** DMOD nanogels did not exhibit substantial pH-responsive behavior, although there appeared to be a critical transition at pH ~4.8, contributed by the remaining carboxylic acid groups.

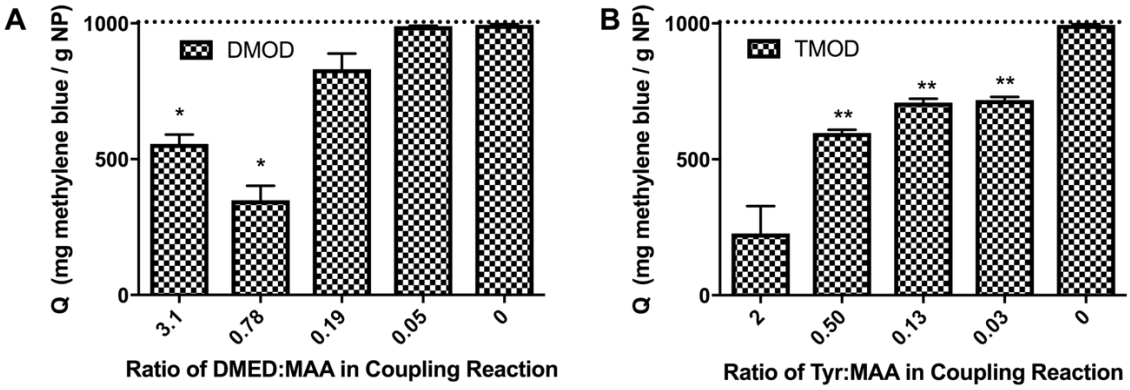

Fig. S6. Methylene blue loading in DMOD and TMOD nanogels. Methylene blue partitioning was measured after 15 min of nanogel incubation with an equivalent quantity of methylene blue in ultrapure water (1 mg/mL nanogels, 1 mg/mL methylene blue). Nanogel modification with either ligand decreased the nanogels' mass loading of methylene blue. The 0.78 DMOD and 0.50 TMOD formulations were used in drug delivery experiments. The dotted line represents complete partitioning of the methylene blue. (n = 3, mean ± SD, *$p < 0.05$, **$p < 0.01$, relative the unmodified polymer. 1-way ANOVA with Tukey posttest).

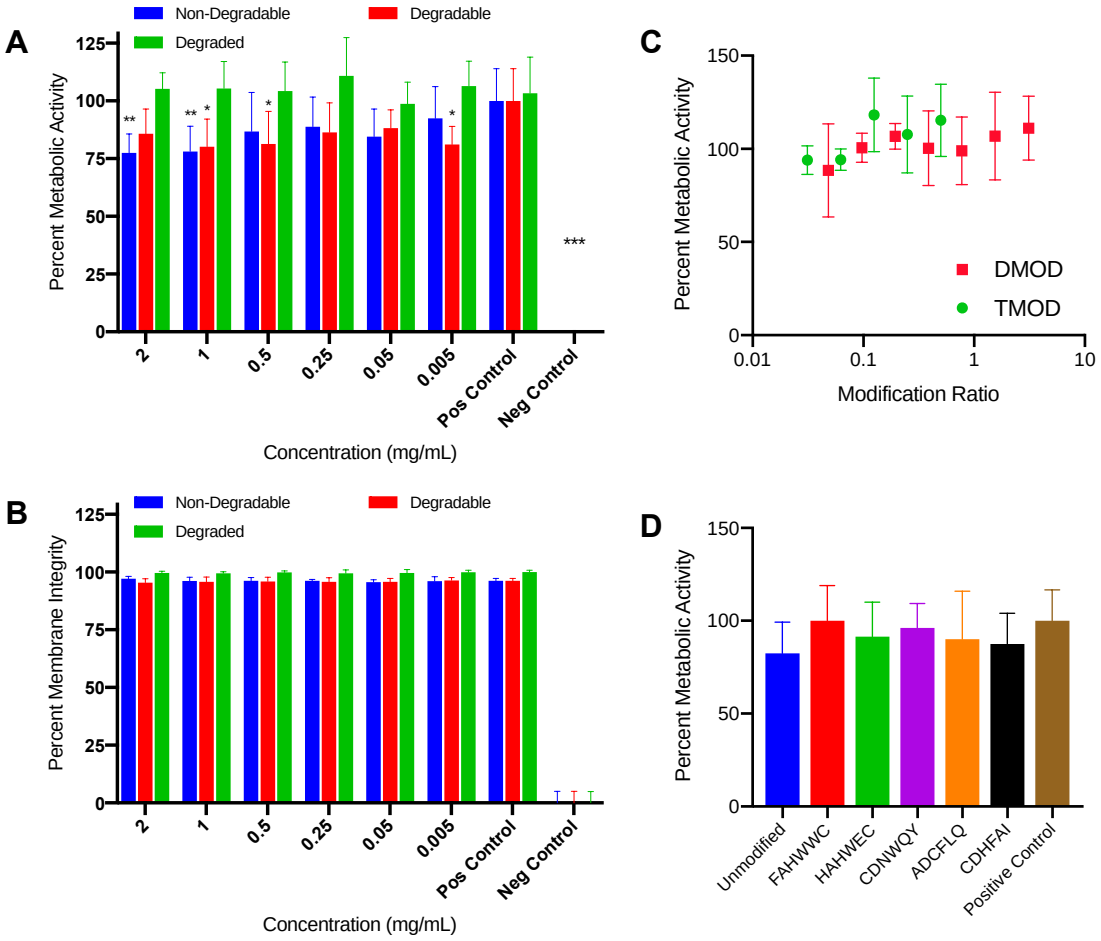

Fig. S7. Nanogel cytotoxicity to murine fibroblasts, as determined by MTS and LDH assays. Presented here are the cytotoxicity data for murine fibroblasts. **(a)** Intact degradable and non-degradable nanogels were acutely toxic to murine fibroblasts at the top concentrations tested (greater than 0.5 mg/mL), as evidenced by metabolic activity. (24 h) **(b)** Fibroblast membrane integrity was relatively unaffected by treatment, indicating that their membranes were not disrupted by nanoparticles. (24 h) **(c)** Modification with N,N-dimethylethylenediamine and/or tyramine did not alter the nanogel cytotoxicity (2 mg/mL treatment, 24 h). **(d)** Peptide modification at 2 wt% did not alter nanogel cytotoxicity, and peptide modified nanogels were non-toxic to fibroblasts (2 mg/mL, 24 h). (n = 6, mean ± SD, *p < 0.05, **p < 0.01, **p < 0.001, 2-way ANOVA with Tukey posttest).

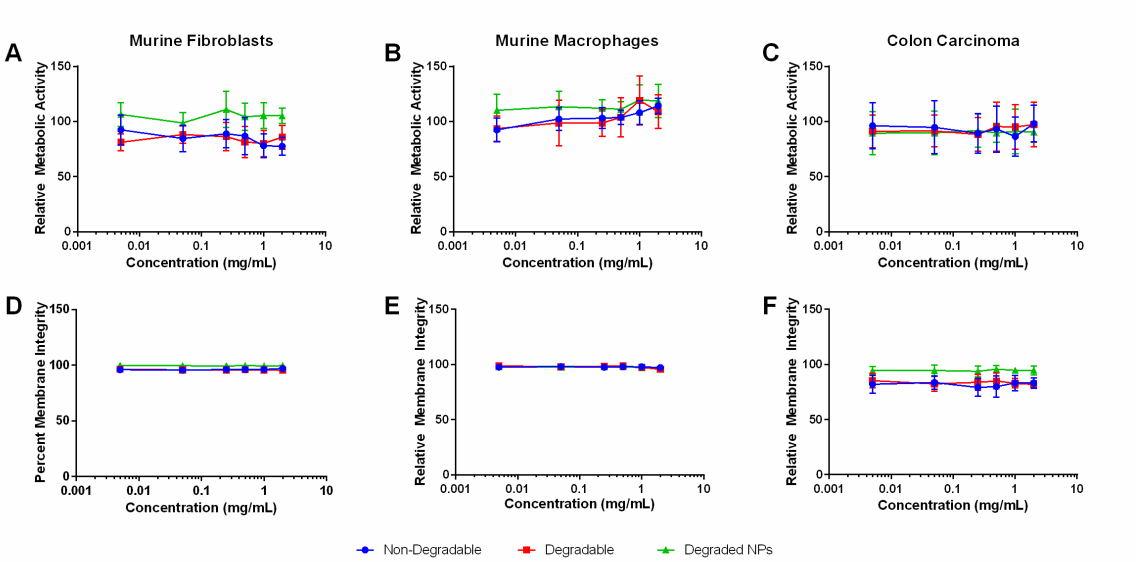

Fig. S8. Cytotoxicity of degradable, nondegradable, and degraded nanogels to fibroblasts, macrophages, and colon epithelial cells. Nanogels were non-toxic to all three cell lines up to 2 mg/mL, as evidenced by cell metabolic activity (MTS assay, panels **a, b, and c)**, and cell membrane integrity (LDH assays, panels **d, e, and f).** Macrophage activation, as evidenced by an increase in metabolic activity relative to control, was observed at nanoparticle concentrations greater than 1 mg/mL. (n = 6, mean ± SD)

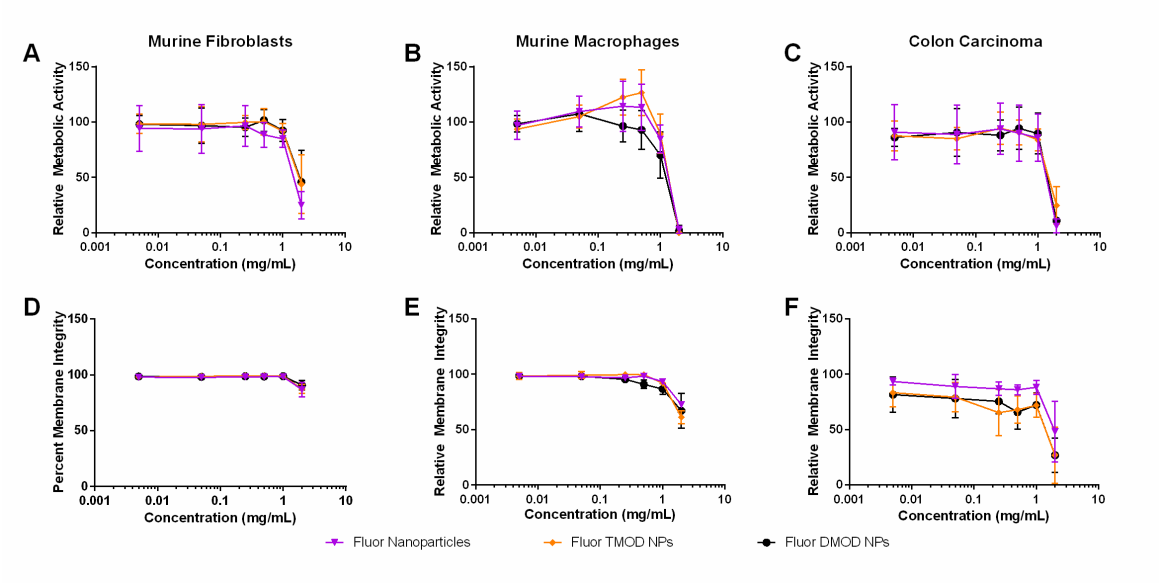

Fig. S9. Cytotoxicity of fluorescent TMOD, DMOD, or unmodified (Fluor) nanogels. Cytotoxicity was determined by quantifying the metabolic activity and membrane integrity of murine fibroblasts, murine macrophages, and human colon epithelial cells after 24 h incubation with nanogels. All formulations were similarly toxic at 2 mg/mL to all three cell lines, as revealed by decreased metabolic activity **(a, b, c)** and a decrease in membrane integrity **(d, e, f).** No significant differences were observed between formulations. Based on these results, we set the maximum dose for cell uptake and imaging experiments at 1 mg/mL nanogels. (n = 6, mean ± SD).

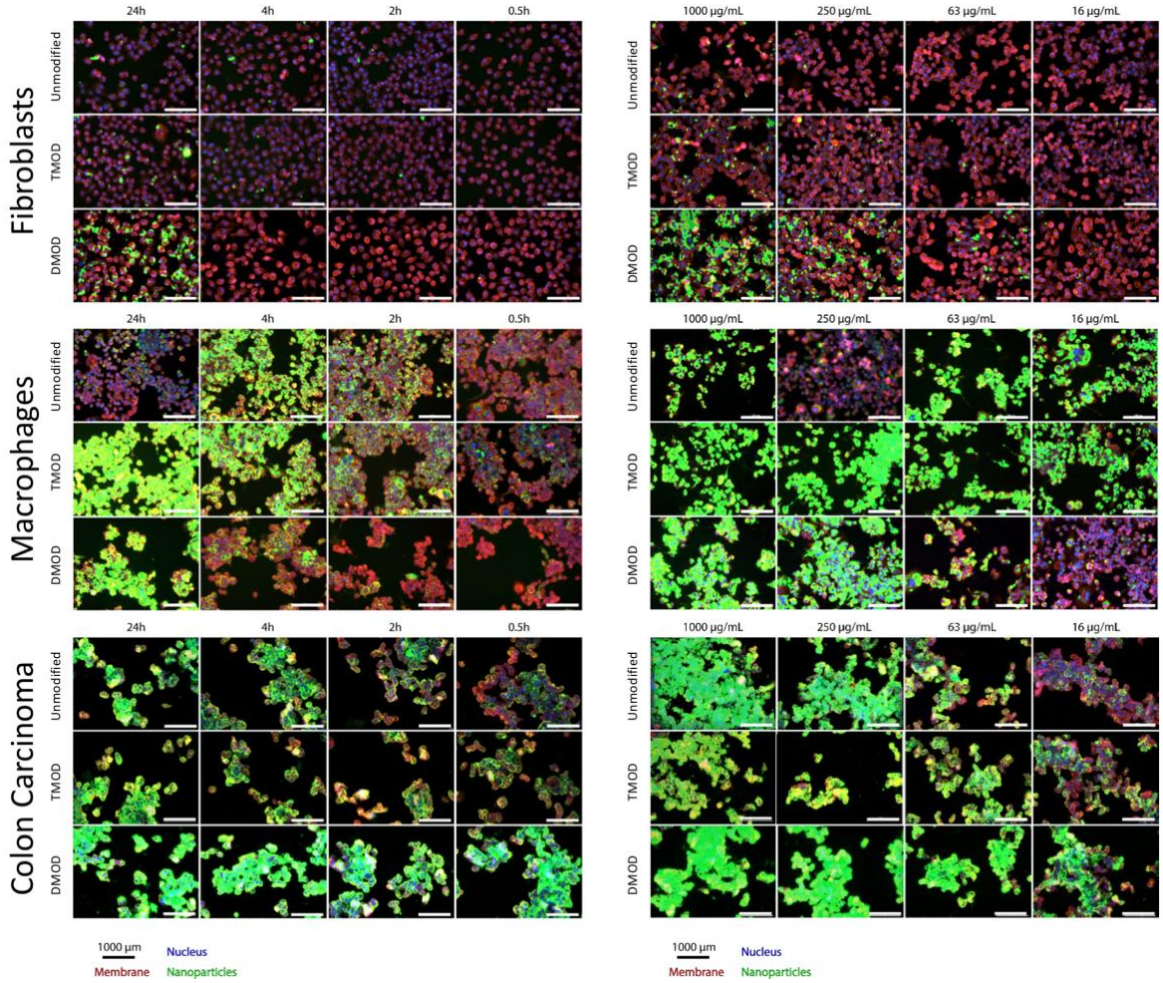

Fig. S10. Representative images for dose-response and kinetic nanogel uptake. Nanogels were incubated with fibroblasts (L929), macrophages, (RAW 264.7) or colon carcinoma cells (SW-48), after which the cells were fixed and stained for fluorescence microscopy. Kinetic analyses (0-24 h incubation, 400 µg/mL dose) and dose-dependent uptake (24 h exposure) are shown for each cell line. Representative images are shown above, which were taken with a Cytation 3 microplate reader equipped with a 20 x Olympus lens. (Scale bar = 1000 µm, representative images shown).